CHIRALITY

INTRODUCTION

Chiral media have the ability to discriminate between left-handed and right-handed electromagnetic (EM) fields. These media can be classified into two types: (1) isotropic chiral media and (2) structurally chiral media. The molecules of a naturally occurring isotropic chiral medium are handed, while an artificial isotropic chiral medium can be made by randomly dispersing electrically small, handed inclusions (such as springs) in an isotropic achiral host medium. The molecules of a structurally chiral medium, such as a chiral nematic liquid crystal, are randomly positioned but have helicoidal orientational order. Structurally chiral media can also be artificially fabricated either as stacks of uniaxial laminae or using thin-film technology. Whereas considerable theoretical and experimental work on isotropic chiral media has been reported at microwave frequencies during the 1980s and the 1990s, microwave research on structurally chiral media remains in an embryonic stage at the time of this writing (1). Therefore, the major part of this article is devoted to isotropic chiral media.

NATURAL OPTICAL ACTIVITY

Ordinary sunlight is split into its spectral components by a prism. A spectral component is monochromatic (i.e., it has one and only one wavelength λ_0 in vacuum). The wavelength λ_0 of one of the visible spectral components lies anywhere between 400 nm (violet) and 700 nm (red). A spectral component can be *almost* isolated from other spectral components by carefully passing sunlight through a series of filters. Although filtering yields quasimonochromatic light, many experiments have been and continue to be performed and their results analyzed, assuming that the filtered light is monochromatic.

Light is an EM wave with spectral components to which our retinal pigments happen to be sensitive, and the consequent images, in turn, happen to be decipherable in our brains. All optical phenomena can be generalized to other electromagnetic spectral regimes.

Suppose that a monochromatic EM wave is propagating in a straight line in air, which is synonymous with vacuum (or free space) for our present purpose. Its electric field vector vibrates in some direction to which the propagation direction is perpendicular; the frequency of vibration is $f=c/\lambda_0$, where $c=3 \times 10^8$ m/s is the speed of light in vacuum. Its magnetic field vector also vibrates with the same frequency, but is always aligned perpendicular to the electric field vector as well as to the propagation direction. Suppose that we fix our attention on a certain plane that is transverse to the propagation direction. On this plane, the locus of the tip of the electric field vector is the so-called vibration ellipse, which is of the same shape as the locus of the tip of the magnetic field vector. A vibration ellipse is shown in Fig. 1. Its shape is characterized by a tilt angle as well as an axial ratio; in addition, it can be left-handed

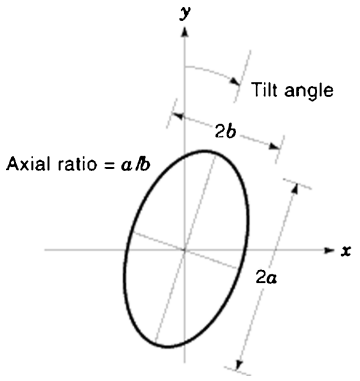

Figure 1. The tip of the electric field vector of a plane-polarized monochromatic electromagnetic wave traces the so–called vibration ellipse in a plane transverse to the propagation direction.

if the tip of the electric field vector rotates counterclockwise, or right-handed if otherwise. Similarly, an EM wave is said to be elliptically polarized, in general; however, the vibration ellipse can occasionally degenerate into a circle (circular polarization) or even a straight line (linear polarization).

The shape of the vibration ellipse of monochromatic light is altered after traversal through a certain thickness of a so-called optically active medium. This phenomenon, known as *optical activity*, was discovered around 1811 by F. Arago while experimenting with quartz. Crystals are generally anisotropic, but J.-B. Biot observed around 1817 the optical activity of turpentine vapor, definitely an isotropic medium. Isotropic organic substances were believed to have exclusively biological provenances, and in 1860 L. Pasteur argued that turpentine vapor exhibited natural optical activity, but the optical activity of crystals could not be similarly qualified. Pasteur was unduly restrictive. Isotropic optically active media, of biological or other origin, are nowadays called *isotropic chiral media*, because EM fields excited in them necessarily possess a property called handedness (Greek *cheir*=hand). Facsimile reproductions of several early papers are available (2).

CHIRAL MEDIA: NATURAL AND ARTIFICIAL

The molecules of an isotropic chiral medium are mirror asymmetric (i.e., they are noncongruent with their mirror images). A chiral molecule and its mirror image are called *enantiomers* (3). As examples, the two enantiomers of 2-butanol are shown in Fig. 2. Enantiomers can have different properties, although they contain identical atoms in identical numbers. One enantiomer of the chiral compound thalidomide may be used to cure morning sickness, during pregnancy, but its mirror image induces fetal malformation. Aspartame, a common artificial sweetener, is one of the four enantiomers of a dipeptide derivative. Of these four, one (i.e., aspartame) is sweet, another is bitter, while the remaining two are tasteless. Of the approximately 1850 natural, semisynthetic, and synthetic drugs marketed these days, no less than 1045 can exist as two or more enantiomers; but only 570 were being marketed in the

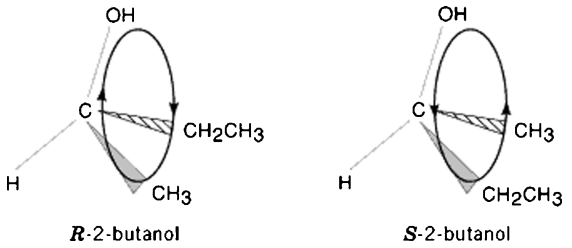

Figure 2. The two enantiomers of 2-butanol are mirror images of each other, as shown by the directed circular arrangements of the –OH, $-CH_2CH_3$, and $-CH_3$ groups.

late 1980s as single enantiomers, of which 61 were totally synthetic. But since 1992, the U.S. Food and Drug Administration (FDA) has insisted that only one enantiomer of a chiral drug be brought into the market. Biological chirospecificity, once the subject of speculations by Pasteur on the nature of the life force (vis viva), is now the topic of conferences on the origin of life (4).

An isotropic chiral medium is circularly birefringent (i.e., both left-handed and right-handed circularly polarized light can propagate in a region filled with a homogeneous isotropic chiral medium, with different phase velocities and attenuation rates). Therefore, when monochromatic, elliptically polarized light irradiates an isotropic chiral slab, the tilt angle and the axial ratio of the transmitted light are different from those of the incident light. The change in the tilt angle is quantified as *optical rotation* (OR) and alteration of the axial ratio as *circular dichroism* (CD). Both OR and CD depend on the wavelength λ_0, and the dependences are reasonably material-specific that spectroscopies based on their measurements have long had industrial importance. Biot himself had pioneered these attempts by cataloging the OR spectra of a large number of syrups and oils, and went on to found the science of saccharimetry for which he was awarded the Rumford Medal in 1840 by the Royal Society of London. The first edition of Landolt's tables on optical activity appeared in the German language in 1879; the English translation of the second edition of 1898 appeared in 1902.

Although Maxwell's unification of light with electromagnetism during the third quarter of the nineteenth century came to mean that natural optical activity is an EM phenomenon, the term *optical rotation* persisted. By the end of the nineteenth century, several empirical rules had evolved on OR spectrums of isotropic chiral mediums. Then, in the late 1890s, two accomplishments of note were reported:

1. J. C. Bose constructed several artificial chiral materials by twisting jute fibers and laying them end to end, and experimentally verified OR at millimeter wavelengths. These materials were anisotropic, but Bose went on to infer from his experiments that isotropic chiral materials could also be constructed in the same way (5). Thus, he conclusively demonstrated the geometric microstructural basis for optical activity, and he also constructed possibly the world's first artificial anisotropic chiral medium to alter the vibration ellipses of microwaves.
2. P. Drude showed that chiral molecules can be modeled as spiral oscillators and theoretically verified a rule Biot had given regarding OR spectra (6).

Experimental verification of Drude's spiral oscillator hypothesis had to wait for another two decades. As electromagnetic propositions can be tested at lower frequencies if the lengths are correspondingly increased and other properties proportionally adjusted, K. F. Lindman made 2.5-turn, 10-mm-diameter springs from 9-cm-long copper wire pieces of 1.2 mm cross-sectional diameter. Springs are handed, as illustrated in Fig. 3. Each spring was wrapped in a cotton ball, and about 700 springs of the same handedness were randomly positioned in a $26\times26\times26$-cm cardboard box with an eye to achieving tolerable isotropy. Then the box was irradiated with 1–3-GHz (30 cm$\geq\lambda_0\geq$10 cm) microwave radiation and the OR was measured. Lindman verified Drude's hypothesis remarkably well. He also determined that (1) the OR was proportional to the number of (identically handed) springs in the box, given that the distribution of springs was rather sparse; and (2) equal amounts of left-handed or right-handed springs brought about the same OR, but in opposite senses (7). Lindman's experiments were extensively repeated during the 1990s by many research groups in several countries (8, 9), and several patents have even been awarded on making artificial isotropic chiral mediums with miniature springs.

CONSTITUTIVE RELATIONS OF AN ISOTROPIC CHIRAL MEDIUM

Electromagnetic fields are governed by the Maxwell postulates, in vacuum as well as in any material medium. These four postulates have a microscopic basis and are given in vacuum as follows:

$$\nabla\cdot\tilde{\boldsymbol{B}}(\boldsymbol{r},t)=0 \tag{1a}$$

$$\nabla\times\tilde{\boldsymbol{E}}(\boldsymbol{r},t)=-\frac{\partial}{\partial t}\tilde{\boldsymbol{B}}(\boldsymbol{r},t) \tag{1b}$$

$$\epsilon_0\nabla\cdot\tilde{\boldsymbol{E}}(\boldsymbol{r},t)=\tilde{\rho}_{\text{tot}}(\boldsymbol{r},t) \tag{1c}$$

$$\nabla\times\tilde{\boldsymbol{B}}(\boldsymbol{r},t)=\mu_0\epsilon_0\frac{\partial}{\partial t}\tilde{\boldsymbol{E}}(\boldsymbol{r},t)+\mu_0\tilde{\boldsymbol{J}}_{\text{tot}}(\boldsymbol{r},t) \tag{1d}$$

Thus, $\tilde{E}(r,t)$ and $\tilde{B}(r,t)$ are the primitive or the fundamental EM fields, both functions of the three-dimensional position vector $\mathbf{r}$ and time t; $\varepsilon_0=8.854\times10^{-12}$ F/m and $\mu_0=4\pi\times10^{-7}$ H/m are, respectively, the permittivity and the permeability of vacuum; $\tilde{\rho}_{\text{tot}}(r,t)$ is the electric charge density and $\tilde{\mathbf{J}}_{\text{tot}}(r,t)$ is the electric current density.

Equations (1a), (1b), (1c) and (1d) apply at any length scale, whereas the charge and the current densities must be specified not continuously but over a set of isolated points. Electromagnetically speaking, matter is nothing but a collection of discrete charged particles in vacuum. As per the Heaviside–Lorentz procedure to get a macroscopic description of continuous matter, spatial averages of all fields and sources are taken, while both $\tilde{\rho}_{\text{tot}}(r,t)$ and $\tilde{\mathbf{J}}_{\text{tot}}(r,t)$ are partitioned into matter-derived and externally impressed components. Then the Maxwell postulates at the

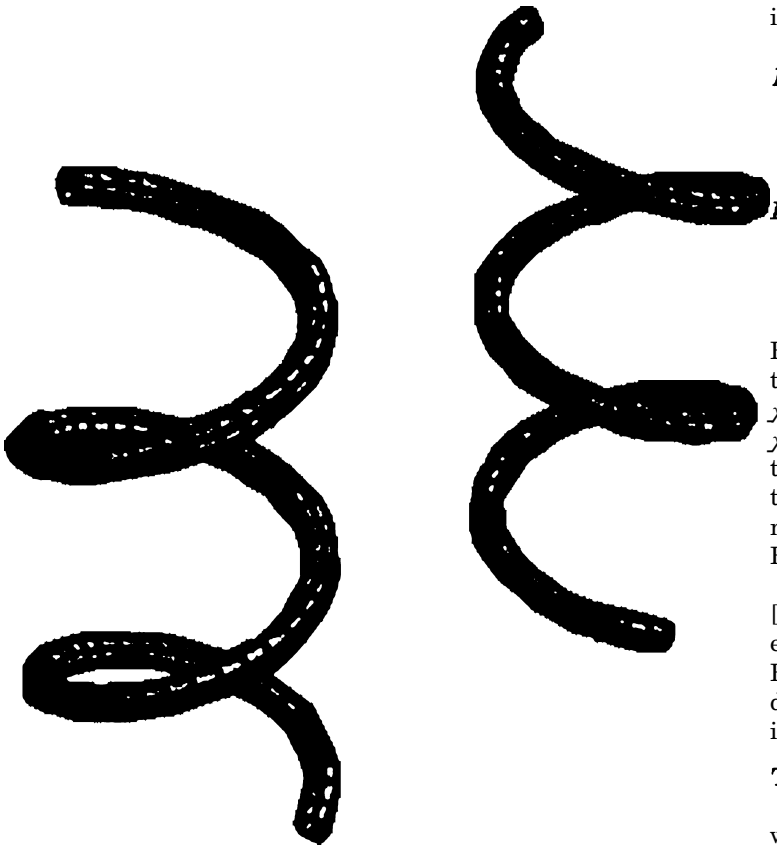

Figure 3. An enantiomeric pair of springs. An artificial isotropic chiral medium can be made by randomly dispersing springs in an isotropic achiral host medium, with more springs of one handedness than the springs of the other handedness.

macroscopic level can be stated as

$$\nabla \cdot \tilde{\boldsymbol{B}}(\boldsymbol{r}, t) = 0 \tag{2a}$$

$$\nabla \times \tilde{\boldsymbol{E}}(\boldsymbol{r}, t) = -\frac{\partial}{\partial t} \tilde{\boldsymbol{B}}(\boldsymbol{r}, t) \tag{2b}$$

$$\nabla \cdot \tilde{\boldsymbol{D}}(\boldsymbol{r}, t) = \tilde{\rho}_{\text{tot}}(\boldsymbol{r}, t) \tag{2c}$$

$$\nabla \times \tilde{\boldsymbol{H}}(\boldsymbol{r}, t) = \frac{\partial}{\partial t} \tilde{\boldsymbol{D}}(\boldsymbol{r}, t) + \tilde{\boldsymbol{J}}(\boldsymbol{r}, t) \tag{2d}$$

Here, $\tilde{\rho}(r, t)$ and $\tilde{J}(r, t)$ are the externally impressed source densities, while the new fields

$$\tilde{\boldsymbol{D}}(\boldsymbol{r}, t) = \epsilon_0 \tilde{\boldsymbol{E}}(\boldsymbol{r}, t) + \tilde{\boldsymbol{P}}(\boldsymbol{r}, t) \tag{3a}$$

$$\tilde{\boldsymbol{H}}(\boldsymbol{r}, t) = [\tilde{\boldsymbol{B}}(\boldsymbol{r}, t) - \tilde{\boldsymbol{M}}(\boldsymbol{r}, t)]/\mu_0 \tag{3b}$$

contain two matter-derived quantities: the polarization $\tilde{P}(r, t)$ and the magnetization $\tilde{\mathrm{M}}(r, t)$

Constitutive relations must be prescribed to relate the matter-derived fields $\tilde{\mathrm{D}}(r, t)$ and $\tilde{\mathrm{H}}(r, t)$ to the basic fields $\tilde{\mathrm{E}}(r, t)$ and $\tilde{\mathrm{B}}(r, t)$ in any material medium. The construction of these relations is primarily phenomenological, although certain epistemologically mandated proprieties must be adhered to. The constitutive relations appropriate for a general, linear, homogeneous, material medium with time-invariant response characteristics may be stated as

$$\tilde{\boldsymbol{D}}(\boldsymbol{r}, t) = \epsilon_0 \tilde{\boldsymbol{E}}(\boldsymbol{r}, t) + \epsilon_0 \int_0^\infty \underline{\tilde{\chi}}^{\mathrm{e}}(\tau) \cdot \tilde{\boldsymbol{E}}(\boldsymbol{r}, t - \tau)\, d\tau + \int_0^\infty \underline{\tilde{\chi}}^{\mathrm{em}}(\tau) \cdot \tilde{\boldsymbol{B}}(\boldsymbol{r}, t - \tau)\, d\tau \tag{4a}$$

$$\tilde{\boldsymbol{H}}(\boldsymbol{r}, t) = \frac{1}{\mu_0} \tilde{\boldsymbol{B}}(\boldsymbol{r}, t) - \frac{1}{\mu_0} \int_0^\infty \underline{\tilde{\chi}}^{\mathrm{m}}(\tau) \cdot \tilde{\boldsymbol{B}}(\boldsymbol{r}, t - \tau)\, d\tau + \int_0^\infty \underline{\tilde{\chi}}^{\mathrm{me}}(\tau) \cdot \tilde{\boldsymbol{E}}(\boldsymbol{r}, t - \tau)\, d\tau \tag{4b}$$

Four constitutive property kernels appear in these equations; the dyadic $\chi^{\mathrm{e}(t)}$ is the dielectric susceptibility kernel, $\chi^{\mathrm{m}(t)}$ is the magnetic susceptibility kernel, while the dyadics $\chi^{\mathrm{em}(t)}$ and $\chi^{\mathrm{em}(t)}$ are called the *magnetoelectric kernels*. Although a dyadic may be understood as a 3×3 matrix for the purpose of this article, Chen's textbook (10) is recommended for a simple introduction to the use of dyadics in EM theory.

All four dyadic kernels in Eqs. (4a) and (4b) are causal [i.e., $\chi^{\mathrm{e}(t)} \equiv \underline{0}\underline{0}$ for $t \leq 0$, etc.], because all materials must exhibit delayed response. In addition, when we substitute Eqs. (4a) and (4b) in Eqs. (2c) and (2d), respectively, a redundancy emerges with respect to Eqs. (2a) and (2b). Elimination of this redundancy leads to the constraint (11)

$$\text{Trace}\,[\underline{\tilde{\chi}}^{\mathrm{em}}(t) - \underline{\tilde{\chi}}^{\mathrm{me}}(t)] \equiv 0 \tag{5}$$

which has never been known to be violated by a physical material. Finally, crystallographic symmetries may also impose additional constraints on the constitutive kernels. A medium described by Eqs. (4a) and (4b) is said to be *bianisotropic*, since the constitutive kernels indicate anisotropy, and both $\tilde{\mathrm{D}}(r, t)$ and $\tilde{\mathrm{H}}(r, t)$ depend on both $\tilde{\mathrm{E}}(r, t)$ and $\tilde{\mathrm{B}}(r, t)$

Suppose next that the linear medium's constitutive properties are direction-independent. Equations (4a) and (4b) then simplify to

$$\tilde{\boldsymbol{D}}(\boldsymbol{r}, t) = \epsilon_0 \tilde{\boldsymbol{E}}(\boldsymbol{r}, t) + \epsilon_0 \int_0^\infty \tilde{\chi}^{\mathrm{e}}(\tau) \tilde{\boldsymbol{E}}(\boldsymbol{r}, t - \tau)\, d\tau + \int_0^\infty \underline{\tilde{\chi}}^{\mathrm{chi}}(\tau) \tilde{\boldsymbol{B}}(\boldsymbol{r}, t - \tau)\, d\tau \tag{6a}$$

$$\tilde{\boldsymbol{H}}(\boldsymbol{r}, t) = \frac{1}{\mu_0} \tilde{\boldsymbol{B}}(\boldsymbol{r}, t) - \frac{1}{\mu_0} \int_0^\infty \underline{\tilde{\chi}}^{\mathrm{m}}(\tau) \tilde{\boldsymbol{B}}(\boldsymbol{r}, t - \tau)\, d\tau + \int_0^\infty \underline{\tilde{\chi}}^{\mathrm{chi}}(\tau) \tilde{\boldsymbol{E}}(\boldsymbol{r}, t - \tau)\, d\tau \tag{6b}$$

in consequence of Eq. (5), where the scalar $\tilde{\chi}^{chi(t)}$ is the chirality kernel. Equations (6a), (6b) describe the *isotropic chiral medium*—the most general, isotropic, linear electromagnetic material known to exist (12, 13).

Most commonly, EM analysis is carried out in the frequency domain, not the time domain. Let all time-dependent quantities be Fourier-transformed; thus

$$\tilde{\boldsymbol{D}}(\boldsymbol{r}, t) = \frac{1}{2\pi} \int_{-\infty}^{\infty} e^{-i\omega t} \boldsymbol{D}(\boldsymbol{r}, \omega)\, d\omega \tag{7}$$

and so on, where $w = 2\ p\ f$ is the angular frequency. In the remainder of this article, phasors such as $D(r, \omega)$ are

called *fields*, following normal practice. The four Maxwell postulates Eqs. (2a), (2b), (2c) and (2d) assume the form

$$\nabla \cdot \boldsymbol{B}(\boldsymbol{r}, \omega) = 0, \tag{8a}$$

$$\nabla \times \boldsymbol{E}(\boldsymbol{r}, \omega) = i\omega \boldsymbol{B}(\boldsymbol{r}, \omega) \tag{8b}$$

$$\nabla \cdot \boldsymbol{D}(\boldsymbol{r}, \omega) = \rho(\boldsymbol{r}, \omega) \tag{8c}$$

$$\nabla \times \boldsymbol{H}(\boldsymbol{r}, \omega) = -i\omega \boldsymbol{D}(\boldsymbol{r}, \omega) + \boldsymbol{J}(\boldsymbol{r}, \omega) \tag{8d}$$

while the constitutive equations [Eqs. 6] for an isotropic chiral medium simultaneously transform into

$$\boldsymbol{D}(\boldsymbol{r}, \omega) = \epsilon_0[1 + \chi^{\mathrm{e}}(\omega)]\boldsymbol{E}(\boldsymbol{r}, \omega) + \chi^{\mathrm{chi}}(\omega)\boldsymbol{B}(\boldsymbol{r}, \omega) \tag{9a}$$

$$\boldsymbol{H}(\boldsymbol{r}, \omega) = \frac{1}{\mu_0}[1 - \chi^{\mathrm{m}}(\omega)]\boldsymbol{B}(\boldsymbol{r}, \omega) + \chi^{\mathrm{chi}}(\omega)\boldsymbol{E}(\boldsymbol{r}, \omega) \tag{9b}$$

Using Eqs. (8b) and (8d) with $\mathbf{J}(\mathbf{r}, \omega) = 0$ in Eqs. (9a) and (9b), respectively, we obtain the Drude–Born–Fedorov (DBF) constitutive relations of an isotropic chiral medium:

$$\boldsymbol{D}(\boldsymbol{r}, \omega) = \epsilon(\omega)[\boldsymbol{E}(\boldsymbol{r}, \omega) + \beta(\omega)\nabla \times \boldsymbol{E}(\boldsymbol{r}, \omega)] \tag{10a}$$

$$\boldsymbol{B}(\boldsymbol{r}, \omega) = \mu(\omega)[\boldsymbol{H}(\boldsymbol{r}, \omega) + \beta(\omega)\nabla \times \boldsymbol{H}(\boldsymbol{r}, \omega)] \tag{10b}$$

Their great merit is that the necessary mirror asymmetry is transparently reflected in them, because $\nabla \times \mathbf{E}(\mathbf{r}, \omega)$ and $\nabla \times \mathbf{H}(\mathbf{r}, \omega)$ are not true vectors but only pseudovectors. A chiral medium is thus described by three constitutive properties; the permittivity and permeability in Eqs. (10a) and (10b), respectively, may be formally defined as the ratios

$$\epsilon(\omega) = \frac{\boldsymbol{D}(\boldsymbol{r}, \omega) \cdot \boldsymbol{E}^*(\boldsymbol{r}, \omega)}{|\boldsymbol{E}(\boldsymbol{r}, \omega)|^2}, \quad \text{if } \boldsymbol{E}^*(\boldsymbol{r}, \omega) \cdot [\nabla \times \boldsymbol{E}(\boldsymbol{r}, \omega)] = 0 \tag{11a}$$

$$\mu(\omega) = \frac{\boldsymbol{B}(\boldsymbol{r}, \omega) \cdot \boldsymbol{H}^*(\boldsymbol{r}, \omega)}{|\boldsymbol{H}(\boldsymbol{r}, \omega)|^2}, \quad \text{if } \boldsymbol{H}^*(\boldsymbol{r}, \omega) \cdot [\nabla \times \boldsymbol{H}(\boldsymbol{r}, \omega)] = 0 \tag{11b}$$

but the chirality parameter $\beta(\omega)$ can be regarded as either

$$\beta(\omega) = \frac{\boldsymbol{D}(\boldsymbol{r}, \omega) \cdot [\nabla \times \boldsymbol{E}^*(\boldsymbol{r}, \omega)]}{\epsilon(\omega)|\nabla \times \boldsymbol{E}(\boldsymbol{r}, \omega)|^2}, \quad \text{if } \boldsymbol{E}(\boldsymbol{r}, \omega) \cdot [\nabla \times \boldsymbol{E}^*(\boldsymbol{r}, \omega)] = 0 \tag{11c}$$

or

$$\beta(\omega) = \frac{\boldsymbol{B}(\boldsymbol{r}, \omega) \cdot [\nabla \times \boldsymbol{H}^*(\boldsymbol{r}, \omega)]}{\mu(\omega)|\nabla \times \boldsymbol{H}(\boldsymbol{r}, \omega)|^2}, \quad \text{if } \boldsymbol{H}(\boldsymbol{r}, \omega) \cdot [\nabla \times \boldsymbol{H}^*(\boldsymbol{r}, \omega)] = 0 \tag{11d}$$

where the asterisk denotes the complex conjugate. Equations (11a), (11b), (11c) and (11d) make it clear that while $\varepsilon(\omega)$ and $\mu(\omega)$ are true scalars, $\beta(\omega)$ has to be a pseudoscalar since the numerator in either of its two definitions contains a pseudovector. Other constitutive relations—equivalent to Eqs. (9a) and (9b) and Eqs. (10a) and (10b)—are also used in the frequency-domain EM literature, but this article is restricted to the DBF constitutive relations Eqs. (10a) and (10b), as they bring out the essence of chirality at the very first glance. An isotropic chiral medium and its mirror image share the same $\varepsilon(\omega)$ and $\mu(\omega)$, and their chirality parameters differ only in sign.

The time-averaged Poynting vector

$$\boldsymbol{S}(\boldsymbol{r}, \omega) = \tfrac{1}{2}\,\mathrm{Real}\{\boldsymbol{E}(\boldsymbol{r}, \omega) \times \boldsymbol{H}^*(\boldsymbol{r}, \omega)\} \tag{12a}$$

denotes the direction of power flow. In any linear medium, the monochromatic Poynting theorem reads as

$$\nabla \cdot \boldsymbol{S}(\boldsymbol{r}, \omega) = -\tfrac{1}{2}\mathrm{Real}\{\boldsymbol{E}(\boldsymbol{r}, \omega) \cdot \boldsymbol{J}^*(\boldsymbol{r}, \omega)\} - \tfrac{1}{2}\mathrm{Real}\{i\omega[\boldsymbol{E}(\boldsymbol{r}, \omega) \cdot \boldsymbol{D}^*(\boldsymbol{r}, \omega) - \boldsymbol{B}(\boldsymbol{r}, \omega) \cdot \boldsymbol{H}^*(\boldsymbol{r}, \omega)]\} \tag{12b}$$

For specialization to an isotropic chiral medium, we have to substitute Eqs. (10a) and (10b) in Eq. (12b). The resulting expression is not particularly illuminating.

An isotropic chiral medium is Lorentz-reciprocal. Suppose that all space is occupied by a homogeneous isotropic chiral medium and all sources are confined to regions of bounded extent. Let sources labeled a radiate fields $\mathbf{E}_a(\mathbf{r}, \omega)$ and $\mathbf{H}_a(\mathbf{r}, \omega)$, while sources labeled b radiate fields $\mathbf{E}_b(\mathbf{r}, \omega)$ and $\mathbf{H}_b(\mathbf{r}, \omega)$, all at the same frequency. Then the relations (12)

$$\nabla \cdot [\boldsymbol{E}_a(\boldsymbol{r}, \omega) \times \boldsymbol{H}_b(\boldsymbol{r}, \omega) - \boldsymbol{E}_b(\boldsymbol{r}, \omega) \times \boldsymbol{H}_a(\boldsymbol{r}, \omega)] = 0 \tag{13a}$$

$$\nabla \cdot [\epsilon(\omega)\boldsymbol{E}_a(\boldsymbol{r}, \omega) \times \boldsymbol{E}_b(\boldsymbol{r}, \omega) - \mu(\omega)\boldsymbol{H}_a(\boldsymbol{r}, \omega) \times \boldsymbol{H}_b(\boldsymbol{r}, \omega)] = 0 \tag{13b}$$

arise in a source-free region, in consequence of the Lorentz reciprocity of the medium.

ARTIFICIAL ISOTROPIC CHIRAL MEDIA

That matter is discrete has long been established. Furthermore, when we probe matter at length scales at which it appears continuous, whether the microstructure is molecular or merely comprises electrically small inclusions is of no consequence. The linear dimensions of an electrically small inclusion are less than about a tenth of the maximum wavelength, in the media outside as well as inside the inclusion, at a particular frequency. Artificial isotropic chiral media—active at microwave frequencies—can be constructed with this thought in mind. Consider a random suspension of identical, electrically small, inclusions in a host medium, which we take here to be vacuum for simplicity. The number of inclusions per unit volume is denoted by N, and the volumetric proportion of the inclusions in the composite medium is assumed to be very small. Our objective is to *homogenize* this dilute particulate composite medium and estimate its effective constitutive properties (13). Homogenization is much like blending apples into apple sauce or tomatoes into ketchup.

Any inclusion scatters the EM wave incident on it. Far away from the inclusion, the scattered EM field phasors can be conceptualized, equivalently, as being radiated by an ensemble of multipoles. Multipoles are necessarily frequency-domain entities; and adequate descriptions of electrically larger inclusions require higher-order multipoles, but homogenizing composite media with electrically large inclusions is fraught with conceptual perils.

The lowest-order multipoles are the electric dipole $\mathbf{p}$ and the magnetic dipole $\mathbf{m}$. In formalisms for isotropic chiral media, both are accorded the same status. As all inclu-

sions in our composite medium are electrically small, we can think that an inclusion located at position $\mathbf{r}'$ is *equivalent* to the colocated dipoles characterized by the following relations:

$$\boldsymbol{p}_{\mathrm{eqvt}}(\boldsymbol{r}', \omega) = \underline{\pi}_{\mathrm{ee}}(\omega) \cdot \boldsymbol{E}_{\mathrm{exc}}(\boldsymbol{r}', \omega) + \underline{\pi}_{\mathrm{eh}}(\omega) \cdot \boldsymbol{H}_{\mathrm{exc}}(\boldsymbol{r}', \omega) \quad (14a)$$

$$\boldsymbol{m}_{\mathrm{eqvt}}(\boldsymbol{r}', \omega) = \underline{\pi}_{\mathrm{he}}(\omega) \cdot \boldsymbol{E}_{\mathrm{exc}}(\boldsymbol{r}', \omega) + \underline{\pi}_{\mathrm{hh}}(\omega) \cdot \boldsymbol{H}_{\mathrm{exc}}(\boldsymbol{r}', \omega) \quad (14b)$$

Here, $\mathbf{E}_{\mathrm{exc}}(\mathbf{r}', \omega)$ and $\mathbf{H}_{\mathrm{exc}}(\mathbf{r}', \omega)$ are the fields *exciting* the particular inclusion; while and $\underline{\pi}_{hh}(\omega)$ are the four linear polarizability dyadics that depend on the frequency, the constitution, and the dimensions of the inclusion. As the inclusions are randomly oriented and any homogenizable chunk of a composite medium contains a large number of inclusions, $\underline{\pi}_{ee}(\omega)$ and other terms in Eqs. (14) can be replaced by their orientationally averaged values. If the homogenized composite medium is isotropic chiral, this orientational averaging process *must* yield

$$\boldsymbol{p}_{\mathrm{eqvt}}(\boldsymbol{r}', \omega) = N[\pi_{\mathrm{ee}}(\omega)\boldsymbol{E}_{\mathrm{exc}}(\boldsymbol{r}', \omega) + i\pi_{\mathrm{chi}}(\omega)\boldsymbol{H}_{\mathrm{exc}}(\boldsymbol{r}', \omega)] \quad (15a)$$

$$\boldsymbol{m}_{\mathrm{eqvt}}(\boldsymbol{r}', \omega) = N[-i\pi_{\mathrm{chi}}(\omega)\boldsymbol{E}_{\mathrm{exc}}(\boldsymbol{r}', \omega) + \pi_{\mathrm{hh}}(\omega)\boldsymbol{H}_{\mathrm{exc}}(\boldsymbol{r}', \omega)] \quad (15b)$$

The polarizability dyadics of electrically small, handed inclusions (e.g., springs) may be computed either with standard scattering methods such as the method of moments (14) or using lumped-parameter circuit models (15). Provided that dissipation in the composite medium can be ignored, at a certain angular frequency, $\pi_{\mathrm{ee}}(\omega)$, $\pi_{\mathrm{hh}}(\omega)$, and $\pi_{\mathrm{chi}}(\omega)$ are purely real-valued.

On applying the Maxwell Garnett homogenization approach, the constitutive relations of the homogenized composite medium (HCM) are estimated as follows (12):

$$\boldsymbol{D}(\boldsymbol{r}, \omega) = \tau_{\mathrm{ee}}(\omega)\boldsymbol{E}(\boldsymbol{r}, \omega) + \tau_{\mathrm{chi}}(\omega)\boldsymbol{H}(\boldsymbol{r}, \omega) \quad (16a)$$

$$\boldsymbol{B}(\boldsymbol{r}, \omega) = \tau_{\mathrm{hh}}(\omega)\boldsymbol{H}(\boldsymbol{r}, \omega) - \tau_{\mathrm{chi}}(\omega)\boldsymbol{E}(\boldsymbol{r}, \omega \quad (16b)$$

where

$$\tau_{\mathrm{ee}}(\omega) = \epsilon_0 + \frac{[9\mu_0 N\pi_{\mathrm{ee}} + 3N^2(\pi_{\mathrm{chi}}^2 - \pi_{\mathrm{ee}}\pi_{\mathrm{hh}})]}{9\epsilon_0\mu_0 - 3N(\epsilon_0\pi_{\mathrm{hh}} + \mu_0\pi_{\mathrm{ee}}) - N^2(\pi_{\mathrm{chi}}^2 - \pi_{\mathrm{ee}}\pi_{\mathrm{hh}})} \quad (16c)$$

$$\tau_{\mathrm{hh}}(\omega) = \mu_0 + \frac{[9\epsilon_0 N\pi_{\mathrm{hh}} + 3N^2(\pi_{\mathrm{chi}}^2 - \pi_{\mathrm{ee}}\pi_{\mathrm{hh}})]}{9\epsilon_0\mu_0 - 3N(\epsilon_0\pi_{\mathrm{hh}} + \mu_0\pi_{\mathrm{ee}}) - N^2(\pi_{\mathrm{chi}}^2 - \pi_{\mathrm{ee}}\pi_{\mathrm{hh}})} \quad (16d)$$

$$\tau_{\mathrm{chi}}(\omega) = \frac{i9\mu_0 N\pi_{\mathrm{chi}}}{9\epsilon_0\mu_0 - 3N(\epsilon_0\pi_{\mathrm{hh}} + \mu_0\pi_{\mathrm{ee}}) - N^2(\pi_{\mathrm{chi}}^2 - \pi_{\mathrm{ee}}\pi_{\mathrm{hh}})} \quad (16e)$$

Equivalently

$$\boldsymbol{D}(\boldsymbol{r}, \omega) = \epsilon_{\mathrm{HCM}}(\omega)[\boldsymbol{E}(\boldsymbol{r}, \omega) + \beta_{\mathrm{HCM}}(\omega)\nabla \times \boldsymbol{E}(\boldsymbol{r}, \omega)] \quad (17a)$$

$$\boldsymbol{B}(\boldsymbol{r}, \omega) = \mu_{\mathrm{HCM}}(\omega)[\boldsymbol{H}(\boldsymbol{r}, \omega) + \beta_{\mathrm{HCM}}(\omega)\nabla \times \boldsymbol{H}(\boldsymbol{r}, \omega)] \quad (17b)$$

are the DBF constitutive relations of the HCM, with

$$\epsilon_{\mathrm{HCM}}(\omega) = \frac{\tau_{\mathrm{ee}}(\omega)\tau_{\mathrm{hh}}(\omega) + \tau_{\mathrm{chi}}^2(\omega)}{\tau_{\mathrm{hh}}(\omega)} \quad (17c)$$

$$\mu_{\mathrm{HCM}}(\omega) = \frac{\tau_{\mathrm{ee}}(\omega)\tau_{\mathrm{hh}}(\omega) + \tau_{\mathrm{chi}}^2(\omega)}{\tau_{\mathrm{ee}}(\omega)} \quad (17d)$$

$$\beta_{\mathrm{HCM}}(\omega) = -\frac{i}{\omega}\frac{\tau_{\mathrm{chi}}(\omega)}{\tau_{\mathrm{ee}}(\omega)\tau_{\mathrm{hh}}(\omega) + \tau_{\mathrm{chi}}^2(\omega)} \quad (17e)$$

as the constitutive parameters. Clearly, if $\pi_{\mathrm{chi}}(\omega) \neq 0$ the composite medium has been homogenized into an isotropic chiral medium. In passing, other homogenization approaches are also possible for chiral composites (1, 13).

BELTRAMI FIELDS IN AN ISOTROPIC CHIRAL MEDIUM

In a source-free region occupied by a homogeneous isotropic chiral medium, $\rho(\mathbf{r}, \omega) = 0$ and $\mathbf{J}(\mathbf{r}, \omega) = 0$. Equations (8a), (8c), and (10a) and (10b) then show that $\nabla \cdot \mathbf{E}(\mathbf{r}, \omega) = 0$ and $\nabla \cdot \mathbf{H}(\mathbf{r}, \omega) = 0$. Thus all four fields—$\mathbf{E}(\mathbf{r}, \omega)$, $\mathbf{H}(\mathbf{r}, \omega)$, $\mathbf{D}(\mathbf{r}, \omega)$ and $\mathbf{B}(\mathbf{r}, \omega)$—are purely solenoidal. Next, Eqs. (8a), (8b), (8c) and (8d) and (10a) and (10b) together yield the following vector Helmholtz-like equations:

$$\nabla^2 \begin{Bmatrix} \boldsymbol{E}(\boldsymbol{r}, \omega) \\ \boldsymbol{H}(\boldsymbol{r}, \omega) \\ \boldsymbol{D}(\boldsymbol{r}, \omega) \\ \boldsymbol{B}(\boldsymbol{r}, \omega) \end{Bmatrix} + 2\frac{\omega^2\epsilon(\omega)\mu(\omega)\beta(\omega)}{1 - \omega^2\epsilon(\omega)\mu(\omega)\beta^2(\omega)}\nabla \times \begin{Bmatrix} \boldsymbol{E}(\boldsymbol{r}, \omega) \\ \boldsymbol{H}(\boldsymbol{r}, \omega) \\ \boldsymbol{D}(\boldsymbol{r}, \omega) \\ \boldsymbol{B}(\boldsymbol{r}, \omega) \end{Bmatrix} + \frac{\omega^2\epsilon(\omega)\mu(\omega)}{1 - \omega^2\epsilon(\omega)\mu(\omega)\beta^2(\omega)} \begin{Bmatrix} \boldsymbol{E}(\boldsymbol{r}, \omega) \\ \boldsymbol{H}(\boldsymbol{r}, \omega) \\ \boldsymbol{D}(\boldsymbol{r}, \omega) \\ \boldsymbol{B}(\boldsymbol{r}, \omega) \end{Bmatrix} = \begin{Bmatrix} \boldsymbol{0} \\ \boldsymbol{0} \\ \boldsymbol{0} \\ \boldsymbol{0} \end{Bmatrix} \quad (18)$$

In the limit $\beta(\omega) \to 0$ the medium becomes achiral and these equations reduce to the familiar vector Helmholtz equation, and so on.

In lieu of the second-order differential equations [Eqs. (23)], first-order differential equations can be formulated. Thus, after defining the auxiliary fields

$$\boldsymbol{Q}_1(\boldsymbol{r}, \omega) = \frac{1}{2}\left[\boldsymbol{E}(\boldsymbol{r}, \omega) + i\sqrt{\frac{\mu(\omega)}{\epsilon(\omega)}}\boldsymbol{H}(\boldsymbol{r}, \omega)\right] \quad (19a)$$

$$\boldsymbol{Q}_2(\boldsymbol{r}, \omega) = \frac{1}{2}\left[\boldsymbol{H}(\boldsymbol{r}, \omega) + i\sqrt{\frac{\epsilon(\omega)}{\mu(\omega)}}\boldsymbol{E}(\boldsymbol{r}, \omega)\right] \quad (19b)$$

and using the wavenumbers

$$\gamma_1(\omega) = \frac{\omega\sqrt{\epsilon(\omega)\mu(\omega)}}{1 - \omega\beta(\omega)\sqrt{\epsilon(\omega)\mu(\omega)}} \quad (20a)$$

$$\gamma_2(\omega) = \frac{\omega\sqrt{\epsilon(\omega)\mu(\omega)}}{1 + \omega\beta(\omega)\sqrt{\epsilon(\omega)\mu(\omega)}} \quad (20b)$$

we get the two first-order differential equations

$$\nabla \times \boldsymbol{Q}_1(\boldsymbol{r}, \omega) = \gamma_1(\omega)\boldsymbol{Q}_1(\boldsymbol{r}, \omega) \quad (21a)$$

$$\nabla \times \boldsymbol{Q}_2(\boldsymbol{r}, \omega) = -\gamma_2(\omega)\boldsymbol{Q}_2(\boldsymbol{r}, \omega) \quad (21b)$$

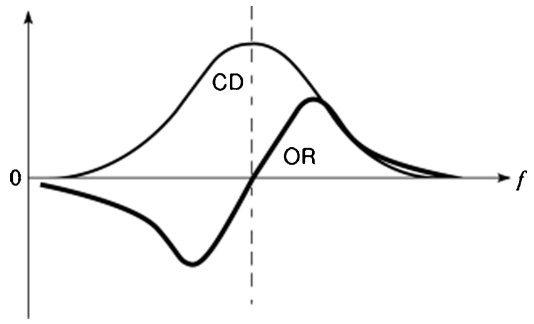

Figure 4. Optical rotation (OR) and circular dichroism (CD) spectra of a simple isotropic chiral medium. When the OR changes sign, the CD records either a maximum or a minimum, which phenomenon is called the *Cotton effect*.

which are easier to analyze than Eqs. (18). The denominators on the left sides of Eqs. (20a) and (20b) suggest that $\omega^2\varepsilon(\omega)\mu(\omega)\beta^2(\omega) = 1$ is not permissible for an isotropic chiral medium, as both wavenumbers must have finite magnitudes.

According to Eqs. (21a) and (21b), $\mathbf{Q}_1(\mathbf{r}, \omega)$ and $\mathbf{Q}_2(\mathbf{r}, \omega)$ are Beltrami fields (12). A Beltrami field is parallel to its own circulation. The concept arose early in the nineteenth century, and has often been rediscovered. The easiest way to think of a Beltrami field is as a spiral staircase or a tornado.

While $\mathbf{Q}_1(\mathbf{r}, \omega)$ is a left-handed Beltrami field, the negative sign on the right side of Eq. (15b) means that $\mathbf{Q}_2(\mathbf{r}, \omega)$ is a right-handed Beltrami field, because the two complex-valued wavenumbers $\gamma_1(\omega)$ and $\gamma_2(\omega)$ must have positive real parts. Both wavenumbers also must have positive imaginary parts in a causal material medium, since causal materials must exhibit delayed response in the time domain and therefore must demonstrate EM loss (or attenuation) in the frequency domain.

As an isotropic chiral medium displays two distinct wavenumbers at a specific frequency, it is *birefringent*. More specifically, because $\mathbf{Q}_1(\mathbf{r}, \omega)$ and $\mathbf{Q}_2(\mathbf{r}, \omega)$ have plane-wave representations possible only in terms of circularly polarized plane waves, an isotropic chiral medium is often said to be *circularly birefringent*. The difference between $\gamma_1(\omega)$ and $\gamma_2(\omega)$ gives rise to *natural optical activity*. While OR is proportional to the *real* part of $[\gamma_1(\omega) - \gamma_2(\omega)]$, CD is proportional to the *imaginary* part of $[\gamma_1(\omega) - \gamma_2(\omega)]$. The OR and CD spectra must be consistent with the Kramers–Kronig relations (16). The CD spectrum has a local maximum or minimum at the frequency where the sign of the OR changes; this feature is labeled as the *Cotton effect* after H. Cotton, who reported it in 1895 (2). The OR and CD spectra of a simple chiral medium are illustrated in Fig. 4.

REPRESENTATION OF BELTRAMI FIELDS

A Beltrami field is represented in terms of toroidal and poloidal fields because the curl of a toroidal field is poloidal and vice versa (17). Thus, the decomposition

$$\boldsymbol{Q}_\nu(\boldsymbol{r}, \omega) = \gamma_\nu(\omega)\nabla \times [\boldsymbol{r}\Psi_\nu(\boldsymbol{r}, \omega)] + (-)^{\nu+1}\nabla \times \nabla \times [\boldsymbol{r}\Psi_\nu(\boldsymbol{r}, \omega)]: \quad \nu = 1, 2 \tag{22}$$

is possible, as the first parts on the right sides of Eqs. (22) are toroidal and the second parts are poloidal. The scalar functions $\Psi_\nu(\mathbf{r}, \omega)$ satisfy the scalar Helmholtz equation as follows:

$$\nabla^2\Psi_\nu(\boldsymbol{r}, \omega) + \gamma_\nu^2(\omega)\Psi_\nu(\boldsymbol{r}, \omega) = 0: \quad \nu = 1, 2 \tag{23}$$

Solutions of Eqs. (23) in the Cartesian, the circular cylindrical, and the spherical coordinate systems are commonplace (18).

Beltrami plane waves propagating in the $+z$ direction may be represented as

$$\boldsymbol{Q}_\nu(\boldsymbol{r}, \omega) = A_\nu 2^{-1/2}[\hat{\boldsymbol{x}} + (-)^{\nu+1} i\hat{\boldsymbol{y}}]\exp[i\gamma_\nu(\omega)z]: \quad \nu = 1, 2 \tag{24}$$

with A_ν as the amplitudes, while $\hat{x}$, $\hat{y}$, and $\hat{z}$ are the Cartesian unit vectors.

In the circular cylindrical coordinate system (ρ, φ, z) Beltrami fields with an $\exp(i\alpha z)$ dependence may be expressed as the sums

$$\boldsymbol{Q}_\nu(\boldsymbol{r}, \omega) = \sum_{n=-\infty}^{\infty} A_{\nu n}[\boldsymbol{M}_n^{(3)}(\gamma_\nu(\omega)|\alpha, \boldsymbol{r}) + (-)^{\nu+1}\boldsymbol{N}_n^{(3)}(\gamma_\nu(\omega)|\alpha, \boldsymbol{r})] \quad \nu = 1, 2 \tag{25a}$$

for regular behavior as $\rho \to \infty$ while the expansions

$$\boldsymbol{Q}_\nu(\boldsymbol{r}, \omega) = \sum_{n=-\infty}^{\infty} B_{\nu n}[\boldsymbol{M}_n^{(1)}(\gamma_\nu(\omega)|\alpha, \boldsymbol{r}) + (-)^{\nu+1}\boldsymbol{N}_n^{(1)}(\gamma_\nu(\omega)|\alpha, \boldsymbol{r})] \quad \nu = 1, 2 \tag{25b}$$

are well behaved at $\rho = 0$ with $A_{\nu n}$ and $B_{\nu n}$ as the coefficients of expansion. The vector cylindrical wavefunctions are given as

$$\boldsymbol{M}_n^{(1)}(\sigma|\alpha, \boldsymbol{r}) = e^{i(\alpha z + n\varphi)}\left[\hat{\boldsymbol{\rho}}\left(\frac{in}{\kappa\rho}\right)J_n(\kappa\rho) - \hat{\boldsymbol{\varphi}}\partial J_n(\kappa\rho)\right] \tag{26a}$$

$$\boldsymbol{M}_n^{(3)}(\sigma|\alpha, \boldsymbol{r}) = e^{i(\alpha z + n\varphi)}\left[\hat{\boldsymbol{\rho}}\left(\frac{in}{\kappa\rho}\right)H_n^{(1)}(\kappa\rho) - \hat{\boldsymbol{\varphi}}\partial H_n^{(1)}(\kappa\rho)\right] \tag{26b}$$

$$\boldsymbol{N}_n^{(j)}(\sigma|\alpha, \boldsymbol{r}) = \frac{1}{\sigma}\nabla \times \boldsymbol{M}_n^{(j)}(\sigma|\alpha, \boldsymbol{r}): \quad j = 1, 3 \tag{26c}$$

where $\kappa = +(\sigma^2 - \alpha^2)^{1/2}$; $\hat{\rho}$, $\hat{\phi}$ and $\hat{z}$ are the unit vectors in the cylindrical coordinate system; $J_n(\kappa\rho)$ are the cylindrical Bessel functions of order n, and $\partial J_n(\kappa\rho)$ are the respective first derivatives with respect to the argument; while $H_n^{(1)}(\kappa\rho)$ are the cylindrical Hankel functions of the first kind and order n, and $H_n^{(1)}(\kappa\rho)$ are the first derivatives with respect to the argument. For quasi-two-dimensional problems, $\alpha = 0$ because $\partial/\partial z = 0$ Parenthetically, in this paragraph ρ denotes the radial distance in the xy plane and should not be confused with the use of ρ for charge density elsewhere in this article.

Finally, with A_{vsmn} and B_{vsmn} as the coefficients of expansion, in the spherical coordinate system $(\mathrm{r}, \theta, \varphi)$, we have

$$\boldsymbol{Q}_\nu(\boldsymbol{r},\,\omega) = \sum_{s=1}^{2}\sum_{n=1}^{\infty}\sum_{m=0}^{n} A_{\nu smn}[\boldsymbol{M}^{(3)}_{smn}(\gamma_\nu(\omega)\boldsymbol{r}) + (-)^{\nu+1}\boldsymbol{N}^{(3)}_{smn}(\gamma_\nu(\omega)\boldsymbol{r})]; \quad \nu = 1,\,2 \tag{27a}$$

for fields regular as $r \to \infty$, and

$$\boldsymbol{Q}_\nu(\boldsymbol{r},\,\omega) = \sum_{s=1}^{2}\sum_{n=1}^{\infty}\sum_{m=0}^{n} \boldsymbol{B}_{\nu smn}[\boldsymbol{M}^{(1)}_{smn}(\gamma_\nu(\omega)\boldsymbol{r}) + (-)^{\nu+1}\boldsymbol{N}^{(1)}_{smn}(\gamma_\nu(\omega)\boldsymbol{r})]; \quad \nu = 1,\,2 \tag{27b}$$

for fields regular at $r = 0$. The well-known vector spherical wavefunctions, $\mathrm{M}^{(j)}_{smn}(\sigma r)$ and $\mathrm{N}^{(j)}_{smn}(\sigma r)$ are stated for $j = 1, 3$ as

$$\boldsymbol{M}^{(1)}_{smn}(\sigma\boldsymbol{r}) = -[n(n+1)]^{1/2} j_n(\sigma r)\hat{\boldsymbol{r}} \times \boldsymbol{B}_{smn}(\theta,\,\phi) \tag{28a}$$

$$\boldsymbol{M}^{(3)}_{smn}(\sigma\boldsymbol{r}) = -[n(n+1)]^{1/2} h^{(1)}_n(\sigma r)\hat{\boldsymbol{r}} \times \boldsymbol{B}_{smn}(\theta,\,\phi) \tag{28b}$$

$$\boldsymbol{N}^{(j)}_{smn}(\sigma\boldsymbol{r}) = \frac{1}{\sigma}\nabla \times \boldsymbol{M}^{(j)}_{smn}(\sigma\boldsymbol{r}): \quad j = 1,\,3 \tag{28c}$$

where the angular functions

$$\boldsymbol{B}_{1mn}(\theta,\,\phi) = [n(n+1)]^{-1/2}\left[\hat{\boldsymbol{\theta}}\frac{d}{d\theta}P^m_n(\cos\theta)\sin m\psi + \hat{\boldsymbol{\psi}}\frac{m}{\sin\theta}P^m_n(\cos\theta)\cos m\psi\right] \tag{29a}$$

$$\boldsymbol{B}_{2mn}(\theta,\,\phi) = [n(n+1)]^{-1/2}\left[\hat{\boldsymbol{\theta}}\frac{d}{d\theta}P^m_n(\cos\theta)\cos m\psi - \hat{\boldsymbol{\psi}}\frac{m}{\sin\theta}P^m_n(\cos\theta)\sin m\psi\right] \tag{29b}$$

have been used. In these expressions, $\hat{r}$, $\hat{\theta}$, and $\hat{\phi}$ are the unit vectors in the spherical coordinate system; $P^m_n(\cos\theta)$ are the associated Legendre functions of order n and degree m; $j_n(\sigma r)$ are the spherical Bessel functions of order n; and $h^{(1)}_n(\sigma r)$ are the spherical Hankel functions of the first kind and order n.

Boundary-value problems involving scattering by isotropic chiral half-spaces, cylinders, and spheres can be analytically solved using Eqs. (24,25a) and (25b), (26a), (26b) and (27b), (27a) and (27b), (28a) and (28b), (29a) and (29b). Boundary-value problems involving more complicated geometries generally require numerical treatment, which necessitates the use of Green functions.

Isotropic chiral waveguides for use at microwave frequencies have been theoretically studied extensively, although no practical realization thereof has yet come to light. Theoretical investigations on propagation in the so-called chirowaveguides generally consist of decomposing the Beltrami fields into axial and transverse components as

$$\boldsymbol{Q}_\nu(\boldsymbol{r},\,\omega) = \boldsymbol{Q}_{\nu t}(\boldsymbol{r},\,\omega) + \hat{\boldsymbol{z}}\boldsymbol{Q}_{\nu z}(\boldsymbol{r},\,\omega), \quad \hat{\boldsymbol{z}}\cdot\boldsymbol{Q}_{\nu t}(\boldsymbol{r},\,\omega) \equiv 0: \quad \nu = 1,\,2, \tag{30}$$

where the z coordinate is measured on the waveguide axis while two other mutually orthogonal coordinates are specified in the transverse plane. Assuming that all fields have an $\exp(i\alpha z)$ dependence on z, and making use of Eqs. (21a) and (21b), we get

$$\boldsymbol{Q}_{\nu t}(\boldsymbol{r},\,\omega) = \frac{1}{\gamma^2_\nu(\omega) - \alpha^2}[i\alpha\underline{\boldsymbol{I}} + (-)^\nu\gamma_\nu(\omega)\hat{\boldsymbol{z}}\times\underline{\boldsymbol{I}}] \cdot\left[\nabla - \hat{\boldsymbol{z}}\frac{\partial}{\partial z}\right]Q_{\nu z}(\boldsymbol{r},\,\omega): \quad \nu = 1,\,2 \tag{31}$$

where $\underline{\boldsymbol{I}}$ is the identity dyadic. The axial components satisfy the reduced scalar Helmholtz equations

$$\left[\nabla^2 - \frac{\partial^2}{\partial z^2} + \gamma^2_\nu(\omega) - \alpha^2\right]Q_{\nu z}(\boldsymbol{r},\,\omega) = 0: \quad \nu = 1,\,2 \tag{32}$$

appropriate solutions of which are commonly worked out in many different ways for waveguides of different cross-sectional geometries (18).

SOURCES IN AN ISOTROPIC CHIRAL MEDIUM

Let us now assume the existence of a magnetic charge density $\rho_\mathrm{m}(r,\,\omega)$ and a magnetic current density $J_\mathrm{m}(r,\,\omega)$, because they assist in the solution of dual problems (19). In addition, let us define the intrinsic impedance $\eta(\omega) = \sqrt{\mu(\omega)/\varepsilon(\omega)}$ as well as the auxiliary wavenumber $k(\omega) = \omega\sqrt{\mu(\omega)/\varepsilon(\omega)}$ and drop the explicit indication of dependences on ω for notational simplicity. Now Eqs. (8), (8b), (8c) and (8d) may be written as

$$\nabla\cdot\boldsymbol{B}(\boldsymbol{r}) = \rho_\mathrm{m}(\boldsymbol{r}), \tag{33a}$$

$$\nabla\times\boldsymbol{E}(\boldsymbol{r}) = i\omega\boldsymbol{B}(\boldsymbol{r}) - \boldsymbol{J}_\mathrm{m}(\boldsymbol{r}) \tag{33b}$$

$$\nabla\cdot\boldsymbol{D}(\boldsymbol{r}) = \rho(\boldsymbol{r}) \tag{33c}$$

$$\nabla\times\boldsymbol{H}(\boldsymbol{r}) = -i\omega\boldsymbol{D}(\boldsymbol{r}) + \boldsymbol{J}(\boldsymbol{r}) \tag{33d}$$

which yield the relations

$$\nabla\times\boldsymbol{Q}_\nu(\boldsymbol{r}) + (-)^\nu\gamma_\nu\boldsymbol{Q}_\nu(\boldsymbol{r}) = \boldsymbol{W}_\nu(\boldsymbol{r}): \quad \nu = 1,\,2 \tag{34}$$

for a chiral medium, where

$$\boldsymbol{W}_1(\boldsymbol{r}) = \frac{\gamma_1}{2k}[i\eta\boldsymbol{J}(\boldsymbol{r}) - \boldsymbol{J}_\mathrm{m}(\boldsymbol{r})] \tag{35a}$$

$$\boldsymbol{W}_2(\boldsymbol{r}) = \frac{\gamma_2}{2k}\left[\boldsymbol{J}(\boldsymbol{r}) + \frac{1}{i\eta}\boldsymbol{J}_\mathrm{m}(\boldsymbol{r})\right] \tag{35b}$$

are the Beltrami source current densities (12).

Since Eqs. (34) are linear, they can be solved using standard techniques. Their complete solution can be compactly stated for all $\mathbf{r}$ as

$$\boldsymbol{Q}_\nu(\boldsymbol{r}) = \boldsymbol{Q}^\mathrm{cf}_\nu(\boldsymbol{r}) + \boldsymbol{Q}^\mathrm{rad}_\nu(\boldsymbol{r}): \quad \nu = 1,\,2, \tag{36}$$

where

$$\boldsymbol{Q}^\mathrm{rad}_\nu(\boldsymbol{r}) = (-)^{\nu+1}\frac{2\gamma_1\gamma_2}{k}\int_{V_s}\underline{\boldsymbol{G}}_\nu(\boldsymbol{r},\,\boldsymbol{r}_0)\cdot\boldsymbol{W}_\nu(\boldsymbol{r}_0)d^3\boldsymbol{r}_0: \quad \nu = 1,\,2 \tag{37}$$

are the particular solutions due to the source densities $W_\nu(r)$ which are wholly confined to the region V_s, and $\mathbf{Q}^\mathrm{cf}_\nu(\mathbf{r})$ are the complementary functions satisfying the relations

$$\nabla\times\boldsymbol{Q}^\mathrm{cf}_\nu(\boldsymbol{r}) = (-)^{\nu+1}\gamma_\nu\boldsymbol{Q}^\mathrm{cf}_\nu(\boldsymbol{r}): \quad \nu = 1,\,2 \tag{38}$$

identically. Substituting Eqs. 36–38 in Eqs. (34), we obtain the dyadic differential equations

$$\nabla \times \underline{\boldsymbol{G}}_\nu(\boldsymbol{r}, \boldsymbol{r}_0) + (-)^\nu \gamma_\nu \underline{\boldsymbol{G}}_\nu(\boldsymbol{r}, \boldsymbol{r}_0) = (-)^{\nu+1} \left(\frac{2\gamma_1\gamma_2}{k}\right)^{-1} \underline{\boldsymbol{I}}\delta(\boldsymbol{r} - \boldsymbol{r}_0) \qquad \nu = 1, 2, \tag{39}$$

where $\delta(\cdot)$ is the Dirac delta function.

The solutions of Eqs. (39) are the Beltrami–Green dyadic functions

$$\underline{\boldsymbol{G}}_\nu(\boldsymbol{r}, \boldsymbol{r}_0) = (-)^{\nu+1} \left(\frac{2\gamma_1\gamma_2}{k}\right)^{-1} [\nabla \times \underline{\boldsymbol{I}} + (-)^{\nu+1}\gamma_\nu \underline{\boldsymbol{I}}] \cdot \underline{\boldsymbol{G}}_{\text{fs}}(\gamma_\nu|\boldsymbol{r}, \boldsymbol{r}_0) \qquad \nu = 1, 2, \tag{40}$$

wherein

$$\underline{\boldsymbol{G}}_{\text{fs}}(\sigma|\boldsymbol{r}, \boldsymbol{r}_0) = \left(\underline{\boldsymbol{I}} + \frac{\nabla\nabla}{\sigma^2}\right) \frac{\exp(i\sigma|\boldsymbol{r} - \boldsymbol{r}_0|)}{4\pi|\boldsymbol{r} - \boldsymbol{r}_0|} \tag{41}$$

is the familiar dyadic Green function for free space. As the properties of $\underline{\mathbf{G}}_{\text{fs}}(\sigma, \mathbf{r}, \mathbf{r}_0)$ can be found in almost any graduate-level EM textbook (20, 21), those of $\underline{\mathbf{G}}_\nu(\mathbf{r}, \mathbf{r}_0)$ can be easily determined, as illustrated in Ref. 12.

As an example of the use of Eqs. (37), let us consider an electric dipole moment **P**located at the origin: $\mathbf{J}(\mathbf{r}) = -i\omega\mathbf{p}\delta(\mathbf{r})$ and $\mathbf{J}_{\text{m}}(\mathbf{r}) = 0$ The radiated Beltrami fields turn out be

$$\boldsymbol{Q}_1^{\text{rad}}(\boldsymbol{r}) = \frac{\omega^2\mu}{k} \frac{\gamma_1\gamma_2}{k^2} \gamma_1 \underline{\boldsymbol{G}}_1(\boldsymbol{r}, \underline{0}) \cdot \boldsymbol{p}: \quad r > 0 \tag{42a}$$

$$\boldsymbol{Q}_2^{\text{rad}}(\boldsymbol{r}) = i\omega\frac{\gamma_1\gamma_2}{k^2} \gamma_2 \underline{\boldsymbol{G}}_2(\boldsymbol{r}, \underline{0}) \cdot \boldsymbol{p}: \quad r > 0 \tag{42b}$$

which show clearly that the radiation field of a point electric dipole in an isotropic chiral medium consists of left-handed as well as right-handed components. If we have instead a point magnetic dipole **m** located at the origin, the source current densities are specified as $\mathbf{J}(\mathbf{r}) = 0$ and $\mathbf{J}_m(\mathbf{r}) = -i\omega\mathbf{m}\delta(\mathbf{r})$ so that

$$\boldsymbol{Q}_1^{\text{rad}}(\boldsymbol{r}) = i\omega\frac{\gamma_1\gamma_2}{k^2} \gamma_1 \underline{\boldsymbol{G}}_1(\boldsymbol{r}, \boldsymbol{0}) \cdot \boldsymbol{m}: \quad r > 0 \tag{43a}$$

$$\boldsymbol{Q}_2^{\text{rad}}(\boldsymbol{r}) = \frac{\omega^2\epsilon}{k} \frac{\gamma_1\gamma_2}{k^2} \gamma_2 \underline{\boldsymbol{G}}_2(\boldsymbol{r}, 0) \cdot \boldsymbol{m}: \quad r > 0 \tag{43b}$$

are the corresponding radiated Beltrami fields. A major difference between isotropic chiral and achiral media is shown by the two sets of radiated fields, Eqs. (42a), (42b) and (43a), (43b). Without loss of generality, let the source dipole moments be aligned parallel to the z axis. Then, if the dipole moments are radiating in an achiral medium (i.e., β=0), there is no magnetic field due to **p** and there is no electric field due to **m** at any point on the z axis. On the other hand, the wavenumber difference between the left-handed and the right-handed Beltrami fields guarantees that, in an isotropic chiral medium, both $\mathbf{E}^{\text{rad}}(\mathbf{r})$ and $\mathbf{H}^{\text{rad}}(\mathbf{r})$ are not generally null-valued on the z axis, regardless of which one of the two dipole moments is radiating.

Canonical sources of Beltrami fields are possible. If there is a source distribution such that $J(r) \equiv -(1/i\eta)J_{\text{m}}(r)$ for all **r**, then $Q^{\text{rad}}{}_2(r) \equiv \mathbf{0}$ from Eqs. (35a) and (35b) and (37). Likewise, a source distribution containing electric and magnetic current densities in the simple proportion $J(r) = (1/i\eta)J_{\text{m}}(r)$ for all **r** radiates only a right-handed field, because $Q^{\text{rad}}{}_1(r) \equiv \mathbf{0}$ emerges from the same equations.

Radiation by complex sources has to be generally treated using integral equations. Both the Maue and the Pocklington integral equations for radiation in a homogeneous isotropic chiral medium are available (12). Cerenkov radiation in an isotropic chiral medium has also been described using Beltrami fields (12).

The foregoing developments make it clear that a description involving differentials of only the first order suffices for monochromatic radiation and propagation in an isotropic chiral medium. True, there are $\nabla\nabla$ terms in $\underline{\mathbf{G}}_1(\mathbf{r}, \mathbf{r}_0)$ and $\underline{\mathbf{G}}_2(\mathbf{r}, \mathbf{r}_0)$ but dyadic Green functions are not fields, being instead solutions of dyadic differential equations.

Finally, although the left-handed and the right-handed Beltrami fields are capable of being independently radiated and propagated as per Eqs. (34), they do indeed couple in an isotropic chiral medium. This coupling takes place only at bimedium boundaries where conditions on the tangential components of $\mathbf{E}(\mathbf{r})$ and $\mathbf{H}(\mathbf{r})$ must be satisfied; that is, the boundary conditions are specified not on $\mathbf{Q}_1(\mathbf{r})$ or $\mathbf{Q}_2(\mathbf{r})$ singly, but on the tangential components of the combinations $E(r) = Q_1(r) - i\eta Q_2(r)$ and $H(r) = Q_2(r) + (1/i\eta)Q_1(r)$.

THEOREMS FOR SCATTERING IN AN ISOTROPIC CHIRAL MEDIUM

Equations 36-39 suffice to set up certain often-used principles for monochromatic scattering and radiation problems, when all space is filled with a homogeneous isotropic chiral medium.

The source–region Beltrami fields can be obtained from Eqs. (37) using the Fikioris approach (22). Let S be the surface of the convex-shaped source region V_{s}, where $\hat{\mathbf{n}}_0$ is the unit outward normal at $r_0 \in S$ (see Fig. 5). Then, Eqs. (37) and (40) yield the following relations:

$$\begin{aligned}\boldsymbol{Q}_\nu^{\text{rad}}(\boldsymbol{r}) = (-)^{\nu+1}\gamma_\nu \Bigg\{ \int_{V_{\text{s}}} \Big[\underline{\boldsymbol{G}}_{\text{fs}}(\gamma_\nu|\boldsymbol{r}, \boldsymbol{r}_0) \cdot \boldsymbol{W}_\nu(\boldsymbol{r}_0) \\ - \underline{\boldsymbol{G}}_P(\gamma_\nu|\boldsymbol{r}, \boldsymbol{r}_0) \cdot \boldsymbol{W}_\nu(\boldsymbol{r}) \Big] d^3\boldsymbol{r}_0 - \gamma_\nu^{-2} \underline{\boldsymbol{L}}(\boldsymbol{r}) \cdot \boldsymbol{W}_\nu(\boldsymbol{r}) \Bigg\} \\ + \int_{V_{\text{S}}} [\nabla \times \underline{\boldsymbol{G}}_{\text{fs}}(\gamma_\nu|\boldsymbol{r}, \boldsymbol{r}_0)] \cdot \boldsymbol{W}_\nu(\boldsymbol{r}_0)\, d^3\boldsymbol{r}_0 \\ \nu = 1, 2: \quad \boldsymbol{r} \in V_S\end{aligned} \tag{44}$$

The depolarization dyadic

$$\mathbf{L}(\boldsymbol{r}) = \frac{1}{4\pi} \int_S \frac{\hat{\boldsymbol{n}}_0\boldsymbol{r}_0 - \hat{\boldsymbol{n}}_0\boldsymbol{r}}{|\boldsymbol{r} - \boldsymbol{r}_0|^3}\, d^2\boldsymbol{r}_0 \tag{45}$$

in Eqs. (44) is dependent on the shape of the region V_{s}, while

$$\underline{\boldsymbol{G}}_P(\sigma|\boldsymbol{r}, \boldsymbol{r}_0) = \frac{\nabla\nabla}{\sigma^2} \frac{1}{4\pi|\boldsymbol{r} - \boldsymbol{r}_0|} \tag{46}$$

If the maximum linear extent of the region V_{s} times the magnitude of the greater of the two wavenumbers, γ_1

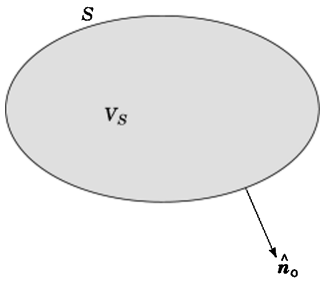

Figure 5. For the evaluation of fields in the region V_s, when the sources are also confined to the same region and all space is occupied by a homogeneous chiral medium.

and γ_2, is much smaller than unity, we may make the quasistatic approximation: $\mathbf{W}_1(\mathbf{r}_0) \cong \mathbf{W}_1(\mathbf{r})$ and $\mathbf{W}_2(\mathbf{r}_0) \cong \mathbf{W}_2(\mathbf{r})$ for all $r_0 \in V_S$. Then, Eqs. (44) simplify to

$$\begin{aligned}\mathbf{Q}_\nu^{\text{rad}}(\mathbf{r}) \cong \{(-)^{\nu+1}\gamma_\nu[\underline{\mathbf{M}}(\gamma_\nu|\mathbf{r}) - \gamma_\nu^{-2}\underline{\mathbf{L}}(\mathbf{r})] \\ + \underline{\mathbf{N}}(\gamma_\nu|\mathbf{r})\} \cdot \boldsymbol{W}_\nu(\mathbf{r}): \quad \nu = 1, 2: \quad \mathbf{r} \in V_S\end{aligned} \tag{47}$$

where the dyadics

$$\underline{\mathbf{M}}(\sigma|\mathbf{r}) = \int_{V_S} [\underline{\mathbf{G}}_{\text{fs}}(\sigma|\mathbf{r}, \mathbf{r}_0) - \underline{\mathbf{G}}_P(\sigma|\mathbf{r}, \mathbf{r}_0)] d^3\mathbf{r}_0 \tag{48a}$$

$$\underline{\mathbf{N}}(\sigma|\mathbf{r}) = \int_{V_S} [\nabla \times \underline{\mathbf{G}}_{\text{fs}}(\sigma|\mathbf{r}, \mathbf{r}_0)] d^3\mathbf{r}_0 \tag{48b}$$

depend on the shape as well as on the size of V_s. Finally, the Rayleigh approximation requires that we ignore the dyadics $\underline{\mathbf{M}}(\sigma|r)$ and $\underline{\mathbf{N}}(\sigma|r)$ completely to obtain the estimates

$$\mathbf{Q}_\nu^{\text{rad}}(\mathbf{r}) \cong (-)^\nu \gamma_\nu^{-1} \underline{\mathbf{L}}(\mathbf{r}) \cdot \boldsymbol{W}_\nu(\mathbf{r}): \quad \nu = 1, 2: \quad \mathbf{r} \in V_S \tag{49}$$

when V_s is an extremely small region. The right sides of Eqs. (47) and (49) are useful in homogenizing isotropic chiral composites as well as for devising the method of moments and the coupled dipole method for scattering by bianisotropic objects in isotropic chiral environments (12, 23).

Turning now to the mathematical realizations of the Huygens principle and its progeny, we suppose that all space is divided into two regions, as shown in Fig. 6. The external region V_{ext} extends to infinity in all directions but is separated from an internal region V_{int} by the convex and once-differentiable surface S. Then the Huygens principle in a homogeneous isotropic chiral medium reads as follows (12):

$$\boldsymbol{Q}_\nu(\mathbf{r}) = (-)^{\nu+1}\frac{2\gamma_1\gamma_2}{k} \int_S \underline{\mathbf{G}}_\nu(\mathbf{r}, \mathbf{r}_0) \cdot [\hat{\boldsymbol{n}}_0 \times \boldsymbol{Q}_\nu(\mathbf{r}_0)] d^2\mathbf{r}_0 \quad \nu = 1, 2: \quad \mathbf{r} \in V_{\text{ext}} \tag{50a}$$

$$\mathbf{0} = \int_S \underline{\mathbf{G}}_\nu(\mathbf{r}, \mathbf{r}_0) \cdot [\hat{\boldsymbol{n}}_0 \times \boldsymbol{Q}_\nu(\mathbf{r}_0: \quad \nu = 1, 2: \quad \mathbf{r} \notin V_{\text{ext}} \tag{50b}$$

Thus, the Cauchy data for the fields in a chiral medium comprise the components of the Beltrami fields that are tangential to a boundary. When these data are prescribed on the surface S, we can find the Beltrami fields everywhere in the region V_{ext}.

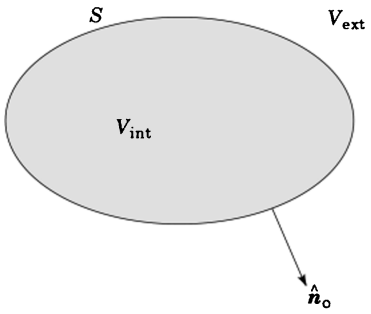

Figure 6. Relevant to the Huygens principle, the exterior surface equivalence principle, and the Ewald–Oseen extinction theorem, when all space is occupied by a homogeneous chiral medium.

The Huygens principle allows the enunciation of the exterior surface equivalence principle. Consider a problem in which surface Beltrami current densities $W^S{}_1(r)$ and $W^S{}_2(r)$ exist on the exterior side of the surface S (see Fig. 6). As per Eqs. (37), these surface current densities act as sources of the radiated fields

$$\boldsymbol{Q}_\nu^{\text{rad}}(\mathbf{r}) = (-)^{\nu+1}\frac{2\gamma_1\gamma_2}{k} \int_S \underline{\mathbf{G}}_\nu(\mathbf{r}, \mathbf{r}_0) \cdot \boldsymbol{W}_\nu^S(\mathbf{r}_0) d^2\mathbf{r}_0 \quad \nu = 1, 2: \quad \mathbf{r} \in V_{\text{ext}} \tag{51}$$

On comparing Eqs. (50a) and (51) to ensure the equivalence $Q^{\text{rad}}{}_\nu(r) \equiv Q_\nu(r)$ for all $r \in V_{\text{ext}}$, we obtain the relationships (12)

$$\boldsymbol{W}_\nu^S(\mathbf{r}_0) = \boldsymbol{n}_0 \times \boldsymbol{Q}_\nu(\mathbf{r}_0): \quad \nu = 1, 2: \quad \mathbf{r}_0 \in S \tag{52}$$

as the exterior surface equivalence principle for Beltrami fields and sources, $\mathbf{r}_0$ in Eqs. (52) lying on the exterior side of S.

The Ewald–Oseen extinction theorem is a cornerstone of the extended-boundary-condition method (12, 24). For scattering in an isotropic chiral medium, this theorem may be stated as

$$\mathbf{0} = \boldsymbol{Q}_\nu^{\text{cf}}(\mathbf{r}) + (-)^{\nu+1}\frac{2\gamma_1\gamma_2}{k} \int_S \underline{\mathbf{G}}_\nu(\mathbf{r}, \mathbf{r}_0) \cdot [\hat{\boldsymbol{n}}_0 \times \boldsymbol{Q}_\nu(\mathbf{r}_0)] d^2\mathbf{r}_0 \quad \nu = 1, 2: \quad \mathbf{r} \in V_{\text{int}} \tag{53}$$

where $Q^{\text{cf}}{}_\nu(r)$ play the role of the incident Beltrami fields. Once $Q_\nu(r_0)$, $r_0 \in S$ have been determined from Eqs. (53), the total fields in the exterior region may be determined as

$$\boldsymbol{Q}_\nu(\mathbf{r}) = \boldsymbol{Q}_\nu^{\text{cf}}(\mathbf{r}) + (-)^{\nu+1}\frac{2\gamma_1\gamma_2}{k} \int_S \underline{\mathbf{G}}_\nu(\mathbf{r}, \mathbf{r}_0) \cdot [\hat{\boldsymbol{n}}_0 \times \boldsymbol{Q}_\nu(\mathbf{r}_0)] d^2\mathbf{r}_0 \quad \nu = 1, 2: \quad \mathbf{r} \in V_{\text{ext}} \tag{54}$$

From Eqs. (53) and (54), the plane-wave scattering dyadics for an object in an isotropic chiral environment can be derived, as can the forward plane-wave scattering amplitude theorems (12).

STRUCTURALLY CHIRAL MEDIA

The molecules of a naturally occurring isotropic chiral medium are mirror-asymmetric, and so are the inclusions in an artificial isotropic chiral medium. As a

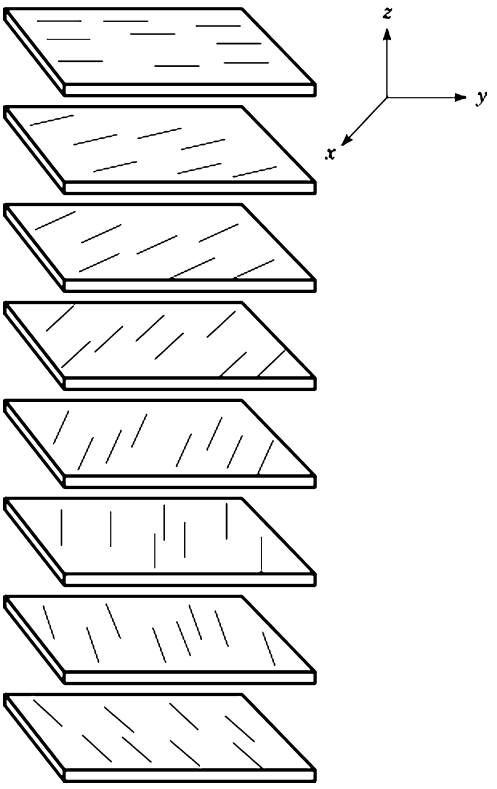

Figure 7. Schematic depiction of the arrangement of needle-like molecules in a chiral nematic liquid crystal. The gaps between the consecutive sheets as well as the sheets are fictitious, as they are merely aids to visualization. Only half of the electromagnetic period is shown.

randomly dispersed and randomly oriented collection of mirror-asymmetric molecules or inclusions is also mirror-asymmetric, isotropic chiral media emerge with direction-independent constitutive properties. In contrast, the molecules or inclusions of a structurally chiral medium are not mirror-asymmetric, but their orientation is.

In chiral nematic liquid crystals (CNLCs)—also called *cholesteric liquid crystals*—needle-like molecules are randomly positioned on parallel sheets, with all molecules on any one sheet oriented parallel to one another and with the orientation rotating helicoidally as one moves across consecutive sheets. The situation is schematically depicted in Fig. 7. From 1850 to 1888, several scientists came across CNLCs but were unable to capitalize on their observations (25). Then in 1888 the biochemist F. Reinitzer observed that a CNLC named *cholesteryl benzoate* has two distinct melting points—it is a solid at temperatures below 145.5°C, a clear liquid at temperatures above 178.5°C, and a cloudy liquid in between. Reinitzer's observation of the mesophase—when positional order is absent as in a liquid, but orientational order is still strong as in a solid—opened up the area of liquid crystal research in continuum mechanics as well as in optics (26–28).

Earlier, however, (in 1869), E. Reusch had anticipated the CNLC structure as a laminate of uniaxial dielectric sheets, with the crystallographic axes of any two adjacent sheets offset in the transverse plane by a fixed small angle. At a low enough frequency, this laminate appears as a continuously nonhomogeneous medium whose constitutive properties vary helicoidally. Thus

$$\boldsymbol{D}(\boldsymbol{r},\,\omega) = \epsilon_0 \underline{\mathbf{S}}(z) \cdot \underline{\epsilon}_{\,\mathrm{ref}}(\omega) \cdot \underline{\mathbf{S}}^{-1}(z) \cdot \boldsymbol{E}(\boldsymbol{r},\,\omega) \tag{55a}$$

$$\boldsymbol{H}(\boldsymbol{r},\,\omega) = \frac{1}{\mu_0}\boldsymbol{B}(\boldsymbol{r},\,\omega) \tag{55b}$$

are the frequency-domain constitutive relations of a CNLC, where

$$\underline{\epsilon}_{\,\mathrm{ref}}(\omega) = \epsilon_a(\omega)[\underline{\mathbf{I}} - \hat{\boldsymbol{z}}\hat{\boldsymbol{z}}] + \epsilon_b(\omega)\hat{\boldsymbol{z}}\hat{\boldsymbol{z}} \tag{56}$$

is the relative permittivity dyadic in a reference plane designated as z=0. The rotation dyadic

$$\underline{\mathbf{S}}(z) = [\hat{\boldsymbol{x}}\hat{\boldsymbol{x}} + \hat{\boldsymbol{y}}\hat{\boldsymbol{y}}]\cos\frac{\pi z}{\Omega} + [\hat{\boldsymbol{y}}\hat{\boldsymbol{x}} - \hat{\boldsymbol{x}}\hat{\boldsymbol{y}}]\sin\frac{\pi z}{\Omega} + \hat{\boldsymbol{z}}\hat{\boldsymbol{z}} \tag{57}$$

denotes that the CNLC structure varies helicoidally in the axial (i.e., z) direction with a period 2 Ω; however, the electromagnetic period is Ω. The upper sign in Eq. (57) applies for structural right-handedness; the lower, for structural left-handedness.

Reusch's model of a CNLC has been often implemented with either uniaxial crystals or fibrous laminae, and appears promising for microwave and RF applications as well (29). More recently, thin-film technology has been pressed into service to realize the CNLC structure by releasing a directed evaporant flux toward a rotating substrate (30, 31). The reference permittivity dyadic of these chiral sculptured thin films (STFs) differs from Eq. (56), being

$$\begin{aligned}\underline{\epsilon}_{\,\mathrm{ref}}(\omega) = {}& \epsilon_a(\omega)[\underline{\mathbf{I}} - (\hat{\boldsymbol{x}}\cos\chi + \hat{\boldsymbol{z}}\sin\chi)(\hat{\boldsymbol{x}}\cos\chi + \hat{\boldsymbol{z}}\sin\chi)] \\ & + \epsilon_b(\omega)(\hat{\boldsymbol{x}}\cos\chi + \hat{\boldsymbol{z}}\sin\chi)(\hat{\boldsymbol{x}}\cos\chi + \hat{\boldsymbol{z}}\sin\chi):\ \chi > 0^\circ\end{aligned} \tag{58}$$

instead, and the electromagnetic period is 2 Ω.

The reference permittivity dyadics in Eqs. (56) and (58) are uniaxial and biaxial, respectively; that is, they have either one or two crystallographic axes. Biaxial $\underline{\varepsilon}_{\mathrm{ref}}(\omega)$ is displayed by chiral smectic liquid crystals also (26, 27). Thus in general $\underline{\varepsilon}_{\mathrm{ref}}(\omega)$ displays orthorhombic symmetry (32). Moreover, particularly with advances in thin-film technology, there is no reason for a chiral STF to be necessarily dielectric only. These considerations led to the proposal of the helicoidal bianisotropic medium (HBM), whose frequency-domain constitutive relations may be stated as (33)

$$\begin{aligned}\boldsymbol{D}(\boldsymbol{r},\,\omega) = {}& \epsilon_0 \underline{\mathbf{S}}(z) \cdot [\mathbf{I} + \underline{\boldsymbol{\chi}}^{\,\mathrm{e}}_{\mathrm{ref}}(\omega)] \cdot \underline{\mathbf{S}}^{-1}(z) \cdot \boldsymbol{E}(\boldsymbol{r},\,\omega) \\ & + \underline{\mathbf{S}}(z) \cdot \underline{\boldsymbol{\chi}}^{\,\mathrm{em}}_{\mathrm{ref}}(\omega) \cdot \underline{\mathbf{S}}^{-1}(z) \cdot \mathbf{B}(\mathbf{r},\,\omega),\end{aligned} \tag{59a}$$

$$\begin{aligned}\boldsymbol{H}(\boldsymbol{r},\,\omega) = {}& \frac{1}{\mu_0}\underline{\mathbf{S}}(z) \cdot [\mathbf{I} - \boldsymbol{\chi}^{\,\mathrm{m}}_{\mathrm{ref}}(\omega)] \cdot \underline{\mathbf{S}}^{-1}(z) \cdot \boldsymbol{B}(\boldsymbol{r},\,\omega) \\ & + \underline{\mathbf{S}}(z) \cdot \chi^{\,\mathrm{me}}_{\mathrm{ref}}(\omega) \cdot \underline{\mathbf{S}}^{-1}(z) \cdot \mathbf{E}(\boldsymbol{r},\,\omega)\end{aligned} \tag{59b}$$

subject to the constraint

$$\mathrm{Trace}[\underline{\boldsymbol{\chi}}^{\,\mathrm{em}}_{\mathrm{ref}}(\omega) - \underline{\boldsymbol{\chi}}^{\,\mathrm{me}}_{\mathrm{ref}}(\omega)] = 0 \tag{60}$$

The launching and propagation of EM waves in HBMs is best studied using a 4×4 matrix differential equation formalism (31, 34).

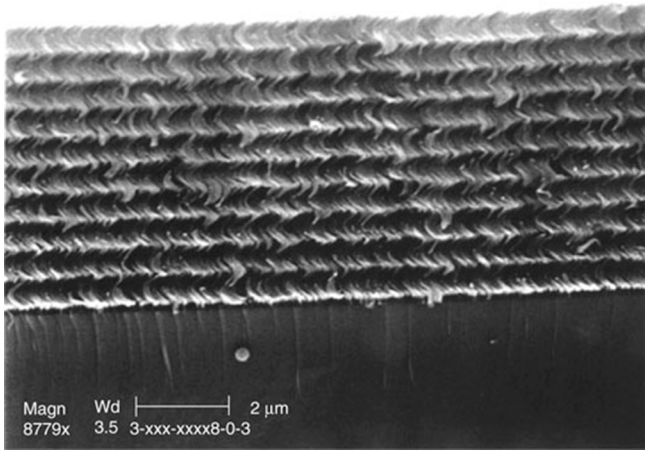

Figure 8. Scanning electron micrograph of a 10-period chiral sculptured thin film made of silicon oxide. (From Professor Russell Messier, Pennsylvania State University, with permission.)

Although chiral STFs made of fluorites, and single-frequency OR measurements on them, were reported in 1959 (35), systematic experimental studies—along with scanning electron microscopic verification of the microstructural geometry—appear to have begun only in 1995 (30). Figure 8 shows the scanning electron micrograph of a chiral STF made of silicon oxide. As typical values of Ω realized today range from 30 nm to 10 μm, microwave applications of these films are yet not feasible, but are likely to become an active area of research once films with $\Omega \sim 100$ μm become available. Many possible applications have been anticipated as the concept of STFs for biological, optical, electronic, chemical, and other applications is beginning to take root, while many optical and related applications have already been implemented (30, 31). Large-scale production appears feasible as well, with adaptation of ion-thruster technology (36).

BIBLIOGRAPHY

1. O. N. Singh andA. Lakhtakia, eds., *Electromagnetic Fields in Unconventional Materials and Structures*, Wiley, New York, 2000.
2. A. Lakhtakia, ed., *Selected Papers on Natural Optical Activity*, SPIE Optical Engineering Press, Bellingham, WA, 1990.
3. J. Jacques, *The Molecule and Its Double*, McGraw-Hill, New York, 1993.
4. B. Holmstedt, F. Hartmut, andB. Testa, eds., *Chirality and Biological Activity*, Alan R. Liss, New York, 1990.
5. J. C. Bose, On the rotation of plane of polarisation of electric waves by a twisted structure, *Proc. Roy. Soc. Lond.* **63**: 146–152 (1898) .
6. P. Drude, *Lehrbuch der Optik*, S. Hirzel, Leipzig, 1900.
7. K. F. Lindman, Über eine durch ein isotropes system von spiralförmigen resonatoren erzeugte rotationspolarisation der elektromagnetischen wellen, *Ann. Phys. Leipzig.* **63**: 621–644 (1920) .
8. R. Ro, Determination of the Electromagnetic Properties of Chiral Composites, Using Normal Incidence Measurements, Ph.D. thesis, Pennsylvania State Univ., University Park, PA, 1991.
9. F. Guérin, Contribution à L'étude Théorique et Expérimentale des Matériaux Composites Chiraux et Bianisotropes dans le Domain Microonde, Ph.D. thesis, Univ. Limoges, Limoges, France, 1995.
10. H. C. Chen, *Theory of Electromagnetic Waves*, TechBooks, Fairfax, VA, 1993.
11. A. Lakhtakia and W. S. Weiglhofer, Constraint on linear, spatiotemporally nonlocal, spatiotemporally nonhomogeneous constitutive relations, *Int. J. Infrared Millim. Waves.* **17**: 1867–1878 (1996) .
12. A. Lakhtakia, *Beltrami Fields in Chiral Media*, World Scientific, Singapore, 1994.
13. A. Lakhtakia, ed., *Selected Papers on Linear Optical Composite Materials*, SPIE Optical Engineering Press, Bellingham, WA, 1996.
14. J. J. H. Wang, *Generalized Moment Methods in Electromagnetics*, Wiley, New York, 1991.
15. C. H. Durney and C. C. Johnson, *Introduction to Modern Electromagnetics*, McGraw-Hill, New York, 1969.
16. A. Moscowitz, Theoretical aspects of optical activity: small molecules, *Adv. Chem. Phys.* **4**: 67–112 (1962) .
17. S. Chandrasekhar, *Hydrodynamic and Hydromagnetic Stability*, Oxford Univ. Press, Oxford, UK, 1961.
18. P. Moon and D. E. Spencer, *Field Theory Handbook*, Springer, Berlin, 1988.
19. R. F. Harrington, *Time-Harmonic Electromagnetic Fields*, McGraw-Hill, New York, 1961, Chapter 3.
20. J. Van Bladel, *Electromagnetic Fields*, Hemisphere Publishing, New York, 1985.
21. W. C. Chew, *Waves and Fields in Inhomogeneous Media*, IEEE Press, New York, 1995.
22. J. G. Fikioris, Electromagnetic field inside a current-carrying region, *J. Math. Phys.* **6**: 1617–1620 (1965) .
23. B. Shanker and A. Lakhtakia, Extended Maxwell Garnett model for chiral-in-chiral composites, *J. Phys. D: Appl. Phys.* **26**: 1746–1758 (1993) .
24. P. C. Waterman, Scattering by dielectric obstacles, Alta Frequenza (Speciale) **38**:348–352 (1969) .
25. P. J. Collings, *Liquid Crystals*, Princeton Univ. Press, Princeton, NJ, 1990, Chapter 2.
26. S. Chandrasekhar, *Liquid Crystals*, Cambridge Univ. Press, Cambridge, UK, 1992.
27. P. G. de Gennes and J. Prost, *The Physics of Liquid Crystals*, Clarendon Press, Oxford, 1993.
28. S. D. Jacobs, ed., *Selected Papers on Liquid Crystals for Optics*, SPIE Optical Engineering Press, Bellingham, WA, 1992.
29. A. Lakhtakia, G. Ya. Slepyan, and S. A. Maksimenko, Towards cholesteric absorbers for microwave frequencies, *Int. J. Infrared Millim. Waves.* **22**: 999–1007 (2001) .
30. A. Lakhtakia, R. Messier, M. J. Brett, and K. Robbie, Sculptured thin films (STFs) for optical, chemical and biological applications, *Innov. Mater. Res.* **1**: 165–176 (1996) .
31. A. Lakhtakia and R. Messier, *Sculptured Thin Films: Nanoengineered Morphology and Optics*, SPIE Press, Bellingham, WA, (2005) .
32. J. F. Nye, *Physical Properties of Crystals*, Clarendon Press, Oxford, 1985.
33. A. Lakhtakia and W. S. Weiglhofer, Axial propagation in general helicoidal bianisotropic media, *Microwave Opt. Technol. Lett.* **6**: 804–806 (1993) .

34. A. Lakhtakia, Director-based theory for the optics of sculptured thin films, *Optik.* **107**: 57–61 (1997) .

35. N. O. Young and J. Kowal, Optically active fluorite films, *Nature.* **183**: 104–105 (1959) .

36. M. W. Horn, M. D. Pickett, R. Messier, and A. Lakhtakia, Blending of nanoscale and microscale in uniform large-area sculptured thin-film architectures, *Nanotechnology* **15**: 303–310 (2004) .

AKHLESH LAKHTAKIA
Pennsylvania State University,
University Park, PA